ICI-Minimizing Blind Uplink Time Synchronization for OFDMA-Based Cognitive Radio Systems

İsmail Güvenç[1], Sibel Tombaz[2], Mustafa E. Şahin[2], Hüseyin Arslan[2], and Hakan Ali Çırpan[3]
[1]DOCOMO Communications Laboratories USA, Inc., 3240 Hillview Avenue, Palo Alto, CA, 94304
[2]Department of Electrical Engineering, University of South Florida, Tampa, FL, 33620
[3]Department of Electrical Engineering, Istanbul University, Avcilar, Istanbul, Turkey
Email: iguvenc@docomolabs-usa.com, sibel.tombaz@boun.edu.tr, msahin@mail.usf.edu, arslan@eng.usf.edu, hcirpan@istanbul.edu.tr

***Abstract*— Cognitive radio is an enabling technology for efficient utilization of radio spectrum. In this paper, an orthogonal frequency division multiple access (OFDMA) based cognitive (opportunistic) network is considered, which co-exists with a macrocell network through utilizing its unused subcarriers. We particularly consider the uplink opportunity detection problem by the opportunistic network, where accurate synchronization to the macrocell network is crucial for minimizing the interference received from the macrocell users. After demonstrating the impact of synchronization on the inter-carrier-interference (ICI) observed at the opportunistic network, an improved blind first-user synchronization technique is proposed, and its statistics are analyzed. Through computer simulations it is shown that the proposed technique yields less interference and better opportunities for the opportunistic network.**

***Index Terms*— Blind synchronization, Cognitive Radio, Femtocell, ICI, Macrocell, OFDMA, Opportunistic Spectrum Access.**

I. Introduction

The tremendous success and growth of wireless devices operating in unlicensed bands have led to the overcrowding of these bands. Cognitive radio has been proposed for more efficient utilization of the wireless spectrum through exploiting the so-called white spaces [1]-[4]. The main idea behind cognitive radio systems is to detect spectrum opportunities in time, frequency, and space, and use these opportunities for communication without causing any significant interference to the license-holder. Some of the recent works also suggest that rather than utilizing the white spaces, through allowing some limited distortion on the primary network (i.e., through utilizing signal-to-noise ratio (SNR) gaps), there is a considerable potential for further improving the spectrum reuse efficiency [5].

In this paper, we consider two wireless networks both of which utilize orthogonal frequency division multiple access (OFDMA) in their physical layers [4]. One of these networks (e.g., a femtocell network) is an opportunistic cognitive network that utilizes the spectrum opportunities available in the other network (e.g., a macrocell network). This requires to reliably sense the spectrum opportunities by minimizing the probability of false alarms (PFA) and probability of missed detections (PMD).

Proper synchronization to the macrocell network carries critical importance for maximizing the spectral opportunities. Uplink (UL) OFDMA signals of the macrocell users arrive at the opportunistic network with different delays. Note that the macrocell users are typically synchronized to their own base stations (BSs) (see e.g., intial/periodic ranging mechanism in WiMAX [6]). However, they arrive at an opportunistic network with different delays, with a spread that linearly increases with the distance between the opportunistic network and the macrocell BS [7]. If any of the macrocell users' signals arrive after the cyclic prefix (CP) of the opportunistic users' signals, this results in inter-symbol interference (ISI) as well as inter-carrier interference (ICI), and may considerably decrease the spectrum opportunities for the opportunistic network [8]. Hence, the opportunistic network should intelligently and blindly (due to absence of direct communication with macrocell users) synchronize to macrocell UL in order to minimize the interference received from the macrocell network.

There are numerous papers related to blind time synchronization for orthogonal frequency division multiplexing (OFDM) systems in the prior art [9]-[14]. However, to our best knowledge, blind synchronization in multiuser interference scenarios has not been addressed in detail in the literature. In [15], a time/frequency synchronization scheme was considered for multiuser OFDM systems, which requires knowledge of each user's subcarrier information, and aims at demodulating the symbols of each of the individual users. However, for an opportunistic network, the subcarrier map of the macrocell users is not available, and its primary goal for synchronization with the macrocell network is to minimize the interference received from the macrocell network, rather than demodulating individual macrocell users' symbols. Even though impact of narrowband interference on synchronization performance has been studied in [16], a pilot-aided timing estimation has been considered rather than a blind approach.

In this paper, we consider over-the-air ICI-minimizing blind synchronization of an opportunistic network to the UL of a macrocell network, without the knowledge of subcarrier allocations of macrocell users. First, it is shown that the ICI power observed at the opportunistic network is typically minimized (or considerably reduced) by synchronizing to the first-arriving UL macrocell user's signal. After reviewing some single-user blind synchronization techniques for OFDM systems, a method that improves the first-user synchronization accuracy is proposed, and its statistics are analyzed in a multiuser setting. Through computer simulations, it is shown that the proposed method reduces the ICI compared to prior-art techniques.

Sibel Tombaz's research is partially supported by the Turkish Scientific and Technical Research Institute (TUBITAK) under grant no. 108E054.

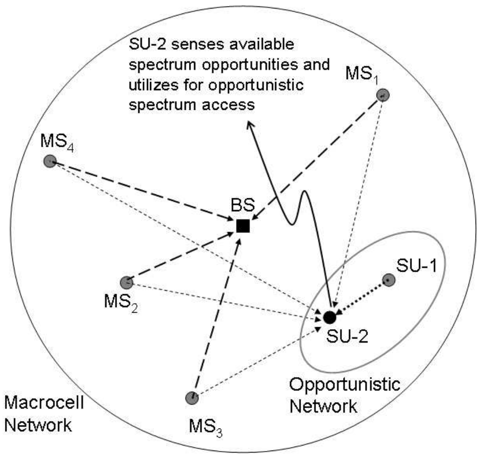

(a) Signals from different macrocell MSs arrive at a secondary device SU-2 (e.g., a femtocell BS) with different delays.

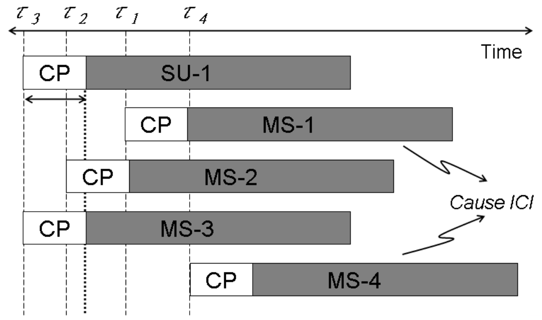

(b) Time domain representation of signal arrival times at SU-2.

Fig. 1. Arrival of macrocell MS signals with different delays at SU-2. Note that macrocell MSs are typically synchronized to their own BS.

The paper is organized as follows. In Section II, system model for UL-OFDMA is presented, impact of synchronization on the performance of an opportunistic network is discussed, and some of the blind OFDM synchronization methods in the prior-art are briefly reviewed. Section III-A derives the statistics of the conventional correlation-based synchronization metric in a multiuser scenario, while Section III-B proposes an improvement for blind first-user synchronization through extending the correlation window length. Section IV provides some related simulation results and the last section concludes the paper.

II. System Model

Consider the macrocell network as in Fig. 1(a), where, multiple mobile stations (MSs) transmit their signals to the macrocell BS in the UL. These signals arrive asynchronously to a secondary user SU-2, where, the arrival time of a signal from the MS$_i$ to the SU-2 is given by τ_i. The time domain representation of the received signals at the SU-2 is illustrated in Fig. 1(b), along with the UL received signal from SU-1. In order to avoid interference from the MSs, the SU-1 should use different subcarriers than all the MSs[1]. Moreover, in order to avoid/minimize ICI received from the macrocell, the signal arrival time of SU-1 at SU-2, denoted by τ_{synch}, should be appropriately designed, which forms the basic motivation for the present work.

[1]If the MSs are very far away from the opportunistic network, their subcarriers may also be reused at the opportunistic network.

A. Signal Model

Since both the macrocell network and the opportunistic network are OFDMA based, their signals can be modeled in the same way. Consider an OFDMA system with N_{u} users in the UL. The sampled time domain signal at the transmitter of user i can be written as

$$x_i^{(m)}(n) = \sqrt{P_{\text{tx},i}} \sum_{k \in \mathbf{\Gamma}_i} X_i^{(m)}(k) e^{\frac{j2\pi kn}{N}} \ , -N_{\text{cp}} \leq n \leq N-1 \ , \tag{1}$$

where m is the symbol index, $P_{\text{tx},i}$ is the total transmitted power per symbol for user i, $k \in \mathbf{\Gamma}_i$ is the subcarrier index, $\mathbf{\Gamma}_i$ is the set of subcarriers assigned to user i out of N total subcarriers, N_{CP} is the length of the cyclic prefix (CP) in samples (and T_{CP} is its length in seconds), and $X_i^{(m)}(k)$ is the data on the kth subcarrier and mth symbol of the ith user.

The time domain aggregate received signal is the superposition of signals from all users, each of which propagates through a different multipath channel and arrives at the receiver with a delay $d_i = \lceil N\tau_i/T \rceil$, where τ_i is the propagation delay experienced by transmitted signal of MS$_i$ and T is the symbol duration in seconds. Then, aggregate discrete-time received signal in the absence of any carrier frequency offset (which we assume negligible in this paper) can be expressed as

$$y(n) = \sum_{i=1}^{N_{\text{u}}} y_i(n - d_i) + w(n), \tag{2}$$

where $w(n)$ denotes the additive white Gaussian noise (AWGN), and

$$y_i(n) = \sqrt{P_{\text{rx},i}} \sum_{l=0}^{L-1} h_i^{(m)}(l) \times \sum_{m=-\infty}^{\infty} x_i^{(m)}\Big(n - D_{l,i} - m(N + N_{\text{CP}})\Big) \ , \tag{3}$$

where L is the total number of multipath components (MPCs), $h_i^{(m)}(l)$ is the amplitude of the lth MPC for user i, and $D_{l,i} = \lceil N\tau_{l,i}/T \rceil$, where $\tau_{l,i}$ is the delay of the lth MPC for user i.

B. Impact of Synchronization Error on the ICI observed at the Opportunistic Network

Timing misalignment between the macrocell UL users and the opportunistic network can lead to significant ICI and limit the amount of available spectrum opportunities for the opportunistic network. Therefore, selection of synchronization point is critically important. If the spread of the MS signals arriving at the opportunistic network is smaller than the CP duration, then the ICI may be totally avoided by synchronizing to the first arriving MS signal, since all the later coming signals will be arriving within the CP duration. However, if the spread of MS signals is larger than the CP duration, synchronization to the first user may not always guarantee minimum ICI. Let $I_i(k)$ denote the ICI signal caused by MS$_i$ on subcarrier k

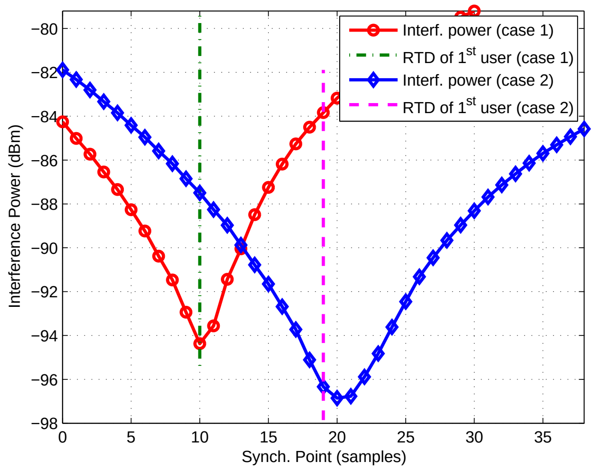

Fig. 2. Effect of the synchronization point on the ICI power. RTD of the first arriving user is close to the optimum synchronization point. Distances of 12 macrocell users to the opportunistic network (in m); case 1: [250, 300, ..., 800]; case 2: [500, 550, ..., 1050].

used by SU-1. Assuming a single occupied subcarrier p_i from each user for notational brevity, the total ICI power observed by SU-2 is given by [17]

$$\sum_{k\neq p_i} I_i^2(k) = \sum_{i=1}^{N_\mathrm{u}} E_{\mathrm{sc},i} \cdot \sum_{k\neq p_i} \frac{1-\cos\left[2\pi(p_i-k)(D_{1,i}-\xi-N_\mathrm{CP})/N\right]}{1-\cos\left[2\pi(p_i-k)/N\right]} \quad (4)$$

where $E_{\mathrm{sc},i}$ is the average received energy per subcarrier for MS_i, and ξ denotes the synchronization point. In [17], it is shown that the ξ that minimizes the ICI, which can be named as optimum ξ, can be obtained by differentiating (4) with respect to ξ and equating it to 0.

In a distance dependent signal power scenario, it can be shown that synchronizing to the first arriving user's signal typically minimizes the ICI in most cases, or makes it sufficiently small. A simple example illustrating this fact is given in Fig. 2, where the amount of total ICI is plotted with respect to the synchronization point for two different scenarios. Free space path loss is assumed with parameters $N = 512$ and $N_\mathrm{CP} = 16$ (i.e., $T_\mathrm{CP} = 2.8$ μs). For the first scenario, the distances of the 12 macrocell users to the opportunistic network are set as $[250, 300, ..., 800]$ m. (corresponding to a round-trip-delay (RTD) difference of 20 samples between the first and last users' signals), whereas in the second scenario they are chosen as $[500, 550, ..., 1050]$ m (corresponding to an RTD difference of 21 samples between first and last users' signals). Since the spread of the signals in both scenarios (20 and 21 samples) is larger than the CP duration (16 samples), there will always be ICI, regardless of the synchronization point. In Fig. 2, it can be seen that if the opportunistic network synchronizes to the first arriving macrocell user signal accurately (i.e., $\tau_\mathrm{synch} = \tau_1$), observed ICI power will be minimum in the first scenario, and considerably close to the minimum in the second scenario. The primary reason for the difference in the second scenario is that first arriving user's signal is attenuated more strongly compared to the first scenario, which makes the contribution of the late arriving signals to the ICI more effective.

C. Review of Blind Time Synchronization Techniques for OFDM Systems

Single user blind synchronization techniques for OFDM systems have been investigated previously in the literature, which will be briefly reviewed here. First, define the following metrics that will be used for synchronization purposes

$$\gamma(\theta) = \sum_{n=\theta}^{\theta+N_\mathrm{CP}-1} y(n)y^*(n+N)\ , \quad (5)$$

$$\phi(\theta) = \sum_{n=\theta}^{\theta+N_\mathrm{CP}-1} y(n)y^*(n)\ . \quad (6)$$

Then, the metrics for timing estimation proposed by Beek (maximum likelihood (ML) metric) [11], Muller [12], Speth (square-difference metric) [13], as well as the simple correlation-based approach are respectively given by

$$f_\mathrm{Beek}(\theta) = |\gamma(\theta)| - \frac{\mathrm{SNR}}{\mathrm{SNR}+1}\,\frac{\phi(\theta)+\phi(\theta+N)}{2}\ , \quad (7)$$

$$f_\mathrm{Muller}(\theta) = |\gamma(\theta)| - \frac{\phi(\theta)+\phi(\theta+N)}{2}\ , \quad (8)$$

$$f_\mathrm{Speth}(\theta) = \sum_{n=\theta}^{\theta+N_\mathrm{CP}-1} |y(n)-y(n+N)|^2\ , \quad (9)$$

$$f_\mathrm{Corr}(\theta) = |\gamma(\theta)|\ . \quad (10)$$

It was shown in [18] that at extremely low signal-to-noise ratios (SNRs), the ML metric is equivalent to the correlation metric, while at high SNRs, ML metric is equivalent to square-difference metric. These methods all aim at synchronizing to an individual user accurately, and demodulate its symbols. However, in order to minimize ICI in a multi-user scenario, as discussed the previous section, accurate first-user synchronization is required.

III. Blind First-User UL Synchronization

In order to understand how the simple correlation based approach in (10) behaves in a multiuser setting, first, its statistics will be derived below. Then, in Section III-B, a simple method for improving the synchronization accuracy through extended correlation window length will be proposed.

A. Statistics of the Conventional Correlation Metric for Multiuser Scenario

Consider the correlation metric in (10) in a multiuser scenario. If we plug the multiuser signal in (2) into the correlation metric (10), we may write

$$\gamma(\theta) = \sum_{n=\theta}^{\theta+N_\mathrm{CP}} y(n)y^*(n+N) \quad (11)$$

$$= \sum_{n=\theta}^{\theta+N_\mathrm{CP}} \left(\sum_{i=1}^{N_\mathrm{u}} y_i(n-d_i)+w(n)\right) \times \left(\sum_{i=1}^{N_\mathrm{u}} y_i(n-d_i+N)+w(n+N)\right)^*\ , \quad (12)$$

which after re-arranging the terms may be re-written as

$$\gamma(\theta) = s_1(\theta) + w_1(\theta) + w_2(\theta) + w_3(\theta) + w_4(\theta) \ , \tag{13}$$

where we have

$$s_1(\theta) = \sum_{n=\theta}^{\theta+N_{\mathrm{CP}}} \sum_{i=1}^{N_{\mathrm{u}}} y_i(n-d_i) y_i^*(n-d_i+N) \ , \tag{14}$$

$$w_1(\theta) = \sum_{n=\theta}^{\theta+N_{\mathrm{CP}}} w(n) \sum_{i=1}^{N_{\mathrm{u}}} y_i^*(n-d_i+N) \ , \tag{15}$$

$$w_2(\theta) = \sum_{n=\theta}^{\theta+N_{\mathrm{CP}}} w^*(n+N) \sum_{i=1}^{N_{\mathrm{u}}} y_i(n-d_i) \ , \tag{16}$$

$$w_3(\theta) = \sum_{n=\theta}^{\theta+N_{\mathrm{CP}}} \sum_{i=1}^{N_{\mathrm{u}}} \sum_{\substack{j=1 \\ j\neq i}}^{N_{\mathrm{u}}} y_i(n-d_i) y_j^*(n-d_j+N) \ , \tag{17}$$

$$w_4(\theta) = \sum_{n=\theta}^{\theta+N_{\mathrm{CP}}} w(n) w^*(n+N) \ . \tag{18}$$

Note that (14) is the desired term in the absence of noise and multi-user interference, while (15)-(18) denote the noise-cross-interference ((15) and (16)), interference-cross-interference, and noise-cross-noise terms, respectively.

The statistics of the noise terms in (15)-(18) can be easily derived as follows[2]

$$\begin{aligned} & w_1(\theta) \sim \mathcal{N}\Big(0, N_{\mathrm{CP}}\sigma_{\mathrm{tot}}^2\Big) \ , \ w_2(\theta) \sim \mathcal{N}\Big(0, N_{\mathrm{CP}}\sigma_{\mathrm{tot}}^2\Big) \ , \\ & w_3(\theta) \sim \mathcal{N}\Big(0, N_{\mathrm{CP}}\sigma_{\mathrm{cross}}^2\Big) \ , \ w_4(\theta) \sim \mathcal{N}\Big(0, N_{\mathrm{CP}}\sigma^4\Big) \ . \end{aligned} \tag{19}$$

where $\sigma_{\mathrm{tot}}^2 = \sigma^2 \sum_{i=1}^{N_{\mathrm{u}}} \tilde{\sigma}_i^2$, $\sigma_{\mathrm{cross}}^2 = \sum_{i=1}^{N_{\mathrm{u}}} \sum_{\substack{j=1 \\ j\neq i}}^{N_{\mathrm{u}}} \tilde{\sigma}_i^2 \tilde{\sigma}_j^2$, and $\tilde{\sigma}_i^2 \doteq P_{\mathrm{rx},i}$. On the other hand, the distribution of the desired term (14) can be written as

$$s_1(\theta) \sim \mathcal{N}\left(\sum_{i=1}^{N_{\mathrm{u}}} E\big\{s_{1,i}(\theta)\big\}, \sum_{i=1}^{N_{\mathrm{u}}} \mathrm{Var}\big\{s_{1,i}\big\} \right) \tag{20}$$

where

$$\mathrm{E}\Big\{s_{1,i}(\theta)\Big\} = \begin{cases} \tilde{\sigma}_i^2 N_{\mathrm{CP}}\Big(1 - \frac{|\theta-d_i|}{N_{\mathrm{CP}}}\Big) & \text{, if } |\theta-d_i| \le N_{\mathrm{CP}} \\ 0 & \text{, otherwise} \ , \end{cases} \tag{21}$$

and

$$\mathrm{Var}\Big\{s_{1,i}(\theta)\Big\} = \begin{cases} \tilde{\sigma}_i^4\big(2N_{\mathrm{CP}} - |\theta-d_i|\big) & \text{, if } |\theta-d_i| \le N_{\mathrm{CP}} \\ \tilde{\sigma}_i^4 N_{\mathrm{CP}} & \text{, otherwise} \ . \end{cases} \tag{22}$$

[2]Note that the true distributions of the variables in (14)-(18) are not Gaussian. However, since they are summations of $N_{\mathrm{CP}}N_{\mathrm{u}}$ random variables ($N_{\mathrm{CP}}N_{\mathrm{u}}^2$ for $w_3(\theta)$), we assume that the true distributions will converge to a Gaussian distribution from the central limit theorem.

B. Improvement of the Correlation Metric for Multiuser Scenario

Note that in (12), the correlation is taken over a duration of N_{CP} OFDM samples. However, in the presence of multiple users, a larger portion of the OFDM symbol will be pairwise correlated, hence requiring a longer correlation window length. Letting the correlation to be taken over a duration of $N_{\mathrm{corr}} = N_{\mathrm{CP}} + D_{\max}$ samples, we may re-write (12) as[3]

$$\begin{aligned} \gamma(\theta) &= \sum_{n=\theta}^{\theta+N_{corr}} y(n) y^*(n+N) & (23) \\ &= \tilde{s}_1(\theta) + \tilde{w}_1(\theta) + \tilde{w}_2(\theta) + \tilde{w}_3(\theta) + \tilde{w}_4(\theta) \ , & (24) \end{aligned}$$

where the statistics of the noise terms become

$$\begin{aligned} & \tilde{w}_1(\theta) \sim \mathcal{N}\Big(0, N_{\mathrm{corr}}\sigma_{\mathrm{tot}}^2\Big) \ , \ \tilde{w}_2(\theta) \sim \mathcal{N}\Big(0, N_{\mathrm{corr}}\sigma_{\mathrm{tot}}^2\Big) \ , \\ & \tilde{w}_3(\theta) \sim \mathcal{N}\Big(0, N_{\mathrm{corr}}\sigma_{\mathrm{cross}}^2\Big) \ , \ \tilde{w}_4(\theta) \sim \mathcal{N}\Big(0, N_{\mathrm{corr}}\sigma^4\Big) \ , \end{aligned} \tag{25}$$

while the distribution of the desired term becomes

$$\tilde{s}_1(\theta) \sim \mathcal{N}\left(\sum_{i=1}^{N_{\mathrm{u}}} E\big\{\tilde{s}_{1,i}(\theta)\big\}, \sum_{i=1}^{N_{\mathrm{u}}} \mathrm{Var}\Big\{\tilde{s}_{1,i}(\theta)\Big\} \right) \ , \tag{26}$$

where

$$\mathrm{E}\Big\{\tilde{s}_{1,i}(\theta)\Big\} = \begin{cases} 0 & , \ \theta \le d_i - N_{\mathrm{corr}} \\ \tilde{\sigma}_i^2 N_{\mathrm{CP}}\Big(1 - \frac{d_i - D_{\max} - \theta}{N_{\mathrm{CP}}}\Big) & , \ d_i - N_{\mathrm{corr}} \le \theta \le d_i - D_{\max} \\ \tilde{\sigma}_i^2 N_{\mathrm{CP}} & , \ d_i - D_{\max} \le \theta \le d_i \\ \tilde{\sigma}_i^2 N_{\mathrm{CP}}\Big(1 - \frac{\theta - d_i}{N_{\mathrm{CP}}}\Big) & , \ d_i \le \theta \le d_i + N_{\mathrm{CP}} \\ 0 & , \ \theta \ge d_i + N_{\mathrm{CP}} \ , \end{cases} \tag{27}$$

$$\mathrm{Var}\Big\{\tilde{s}_{1,i}(\theta)\Big\} = \begin{cases} \tilde{\sigma}_i^4 N_{\mathrm{corr}} & , \ \theta \le d_i - N_{\mathrm{corr}} \\ \tilde{\sigma}_i^4 (2N_{\mathrm{corr}} + \theta - d_i) & , \ d_i - N_{\mathrm{corr}} \le \theta \le d_i - D_{\max} \\ \tilde{\sigma}_i^4 (N_{\mathrm{corr}} + N_{\mathrm{CP}}) & , \ d_i - D_{\max} \le \theta \le d_i \\ \tilde{\sigma}_i^4 (d_i + N_{\mathrm{CP}} - \theta + N_{\mathrm{corr}}) & , \ d_i \le \theta \le d_i + N_{\mathrm{CP}} \\ \tilde{\sigma}_i^4 N_{\mathrm{corr}} & , \ \theta \ge d_i + N_{\mathrm{CP}} \ . \end{cases} \tag{28}$$

Note that noise terms in (25) have larger variances compared to (19) due to a larger correlation window. However, since (27) yields a correlation peak closer to the first user's delay, the synchronization performance (to the first user) will be improved at medium and high SNR scenarios, as will be demonstrated in the next section.

IV. Simulation Results

The performances of the prior art blind synchronization techniques and the proposed method are investigated through computer simulations. First, four different single-user blind synchronization techniques discussed in equations (7)-(10) of Section II-C are simulated and compared in Fig. 3 for completeness, where $d_1 = 32$, $\mathbf{\Gamma}_1 = [-100, ..., -37]$, $N_{\mathrm{CP}} \in$

[3]A typical value for $D_{\max}$ may be set as $d_{N_{\mathrm{u}}} - d_1$.

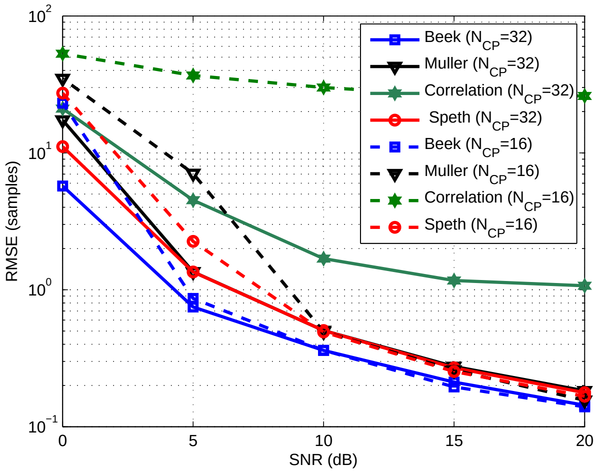

Fig. 3. Comparison of simulated RMSEs of the four different techniques for blind synchronization in a single-user scenario (without averaging).

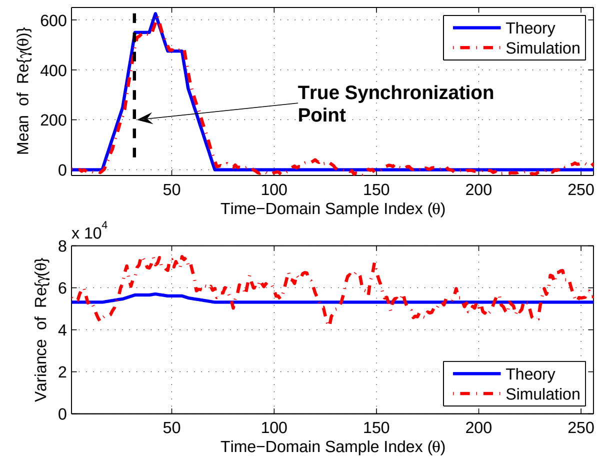

Fig. 5. Comparison of mean and variance of $\mathrm{Re}\{\gamma(\theta)\}$ for $D_{\max} = 0$. Mean of $\mathrm{Re}\{\gamma(\theta)\}$ is maximized at a sample later than the true synchronization instant.

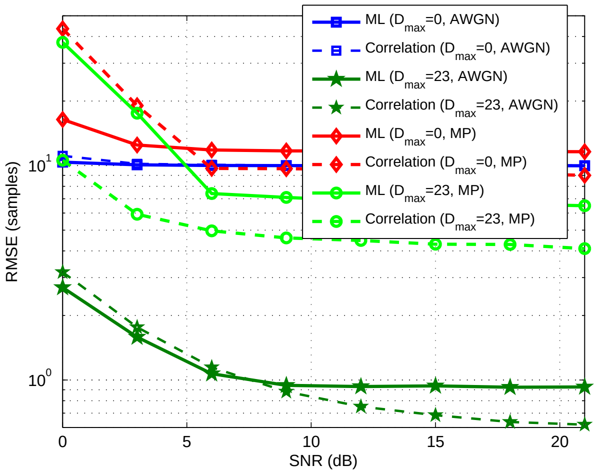

Fig. 4. Comparison of simulated RMSEs of different techniques for blind synchronization in a multi-user scenario ($N_{\mathrm{avg}} = 21,\ N_{\mathrm{CP}} = 32$).

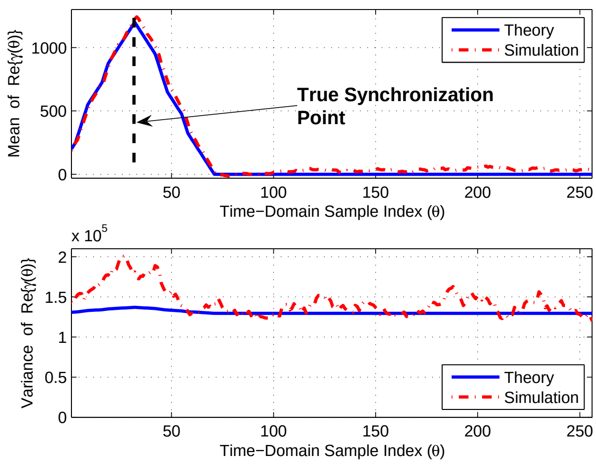

Fig. 6. Comparison of mean and variance of $\mathrm{Re}\{\gamma(\theta)\}$ for $D_{\max} = d_3 - d_1 = 23$. Mean of $\mathrm{Re}\{\gamma(\theta)\}$ is maximized at the true synchronization instant.

$\{16, 32\}$, and $N = 256$ (AWGN channel is considered). As observed from the figure, Beek's ML estimator gives the best result. At high SNRs, Speth's square difference estimator and Muller's estimator both converge to the ML estimator's performance. On the other hand, correlation estimator performs worst among all the techniques. All the former three estimators show marginal improvements when the CP size is increased, while the correlation estimator's performance gets significantly better.

Next, a three-user scenario is considered, where $d_1 = 32$, $d_2 = 42$, and $d_3 = 55$, all in samples, with subcarrier allocation vectors $\mathbf{\Gamma}_1 = [-100, ..., -37]$, $\mathbf{\Gamma}_2 = [-20, ..., 43]$, $\mathbf{\Gamma}_1 = [50, ..., 113]$, $N_{\mathrm{CP}} = 32$, and $N = 256$ (both AWGN and multipath channels (6-tap ITU-R vehicular-A channel model) are considered). In Fig. 4, simulated root mean square errors (RMSEs) of the ML (7) and correlation (10) based approaches for first-user synchronization are illustrated in a for different $D_{\max}$ values. Both synchronization metrics are averaged over $N_{\mathrm{avg}} = 21$ symbols to suppress noise. For all SNR values, setting $D_{\max}$ to $d_3 - d_1 = 23$ samples yields considerably better performance in AWGN channels and some improvements in multipath channels. Hence, single-user ML metric becomes no longer optimal for first-user blind synchronization in a multiuser setting, and using a simple correlation-based approach yields similar or better RMSEs. Further improvements may be possible through more sophisticated techniques that specifically consider the statistics of the MS signal arrival times at SU-2 (see e.g., [7]), which is left as a future work.

Comparison of theoretical and simulated statistics of $\mathrm{Re}\{\gamma(\theta)\}$ for two different $D_{\max}$ values are illustrated in Fig. 5 and Fig. 6 for SNR=20 dB. The three-user scenario with parameters used in Fig. 4 is considered. In Fig. 5, mean and variance of $\mathrm{Re}\{\gamma(\theta)\}$ for $D_{\max} = 0$ (see (21) and (22)) are plotted (i.e., the conventional approach). The mean of the correlation function shows that the peak is achieved at a sample that is later than the true synchronization point of the first user. In Fig. 6, mean and variance of $\mathrm{Re}\{\gamma(\theta)\}$ for $D_{\max} = d_3 - d_1 = 23$ samples (see (27) and (28)) are plotted. As opposed to the scenario when using $D_{\max} = 0$ (i.e., $N_{\text{corr}} = N_{\text{CP}}$), it is observed that using an appropriate larger correlation window as in Fig. 6 results in a correlation function that has a single peak appearing at the true time delay of the first arriving user. Considering that the proposed method has a larger variance, it is expected to perform worse at low-SNRs and better in medium and high SNRs. This may also be observed in Fig. 4, where the degradation in the RMSE performance at low SNRs is worse for $D_{\max} = 23$ compared to $D_{\max} = 0$.

Finally, Fig. 7 shows the spectrum sensing error probability with energy detection, computed as the sum of the PFA (defined as the ratio of the number of subcarriers detected as used although they are unused to N) and PMD (defined as the ratio of number of subcarriers detected as unused although they are used to N). It is assumed that the delays of the 12 macrocell users signals are uniformly distributed within $[\tau_{\min}, \tau_{\max}]$, where, maximum delay $\tau_{\max}$ may be as large as 60 μs. Two different case studies are considered: 1) $\tau_{\min} = 0.25 \times \tau_{\max}$, and 2) $\tau_{\min} = 0.8 \times \tau_{\max}$. Since the spread of the macrocell users' signals is lower in the second case, it is expected that the ICI will be lower, resulting in smaller error probabilities. The results in Fig. 7 confirm this intuition, where the sensing results in Case-2 are considerably better than the sensing results in Case-1. Moreover, synchronization through the proposed method yields lower error probabilities (i.e., lower ICI) compared to the conventional correlation based estimator.

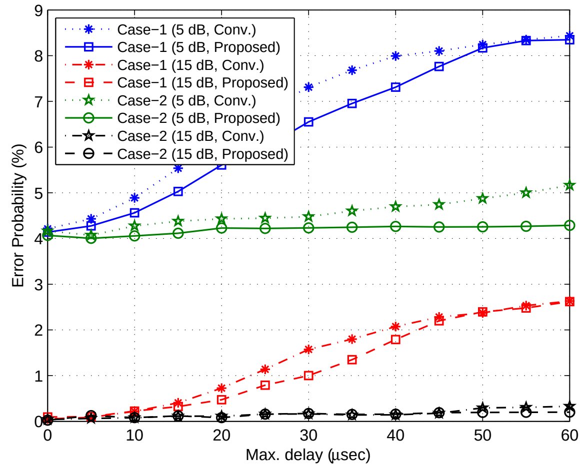

Fig. 7. Performance improvement of spectrum sensing with the proposed synchronization algorithm over correlation based conventional synchronization ($D_{\max} = 0$) and timing misalignment scenarios.

V. Conclusion

In this paper, we analyze how the ICI observed at an opportunistic network relates to the synchronization point and argue that synchronizing to the first arriving UL MS signal minimizes the ICI in most scenarios. Then, a simple extension is proposed for the conventional correlation based blind OFDM synchronization technique, and its statistics are analyzed. Proposed method can be employed for synchronizing OFDMA-based cognitive radio networks, where an opportunistic network (e.g., a femtocell network) tries to utilize the spectrum opportunities available in a primary network. Our future work includes investigation of more accurate synchronization techniques for the scenario in consideration, and obtaining an analytical framework that relate the spectrum opportunities directly with the synchronization method employed.

References

[1] B. Zayen, A. Hayar, and D. Nussbaum, "Blind spectrum sensing for cognitive radio based on model selection," in *Proc. IEEE Cognitive Radio Oriented Wireless Networks and Communications (CrownCom)*, vol. 2, Singapore, May. 2008, pp. 1–4.

[2] R. Chen, J.-M. Park, and K. Bian, "Robust distributed spectrum sensing in cognitive radio networks," in *Proc. IEEE Int. Conf. Comput. Commun. (INFOCOM)*, vol. 2, Phoneix, AR, Apr. 2008, pp. 1876–1884.

[3] S. Mishra, A. Sahai, and R. Brodersen, "Cooperative sensing among cognitive radios," in *Proc. IEEE Int. Conf. Commun. (ICC)*, Istanbul, Turkey, June 2006, pp. 1658–1663.

[4] H. Mahmoud, T. Yucek, and H. Arslan, "OFDM for cognitive radio: merits and challenges," *IEEE Wireless Commun.*, vol. 16, no. 2, pp. 6–15, Apr. 2009.

[5] W. Zhang and U. Mitra, "Exploiting spectral shaping for cognitive radio," in *Proc. Information Theory and Applications Workshop (ITA)*, San Diego, CA, Feb. 2009.

[6] "IEEE 802.16e standard," Feb. 2006. [Online]. Available: http://www.ieee802.org/16/pubs/80216e.html

[7] I. Guvenc, "Statistics of macrocell-synchronous femtocell-asynchronous users' delays for improved femtocell uplink receiver design," *IEEE Commun. Lett.*, vol. 13, no. 4, Apr. 2009.

[8] M. E. Sahin, I. Guvenc, M. R. Jeong, and H. Arslan, "Opportunity detection for OFDMA systems with timing misalignment," in *Proc. IEEE Global Telecommun. Conf. (GLOBECOM)*, New Orleans, LA, Nov. 2008, pp. 1–6.

[9] M. Tanda, "Blind symbol-timing and frequency-offset estimation in OFDM systems with real data symbols," *IEEE Trans. Commun.*, vol. 52, no. 10, pp. 1609–1612, Oct. 2004.

[10] H. Guo, Q. Cheng, and R. Liyana-Pathirana, "Performance comparison of blind symbol timing estimation in cyclic prefixed OFDM systems," in *Proc. IEEE Int. Conf. Technology Enabling Tomorrow: Computers, Communications and Automation (TENCON)*, Melbourne, Australia, Nov. 2005, pp. 1–5.

[11] J. V. Beek, M. Sandell, and P. Borjesson, "ML estimation of time and frequency offset in OFDM systems," *IEEE Trans. Sig. Processing*, vol. 45, no. 7, pp. 1800–1805, July 1997.

[12] S. Muller-Weinfurtner, "On the optimality of metrics for coarse frame synchronization in OFDM: A comparison," in *Proc. IEEE Int. Symp. Personal, Indoor, Mobile Radio Commun. (PIMRC)*, Boston, MA, Sep. 1998.

[13] M. M. Speth, F. Classen, and H. Meyr, "Frame synchronization OFDM systems in frequency selective fading channels," in *Proc. IEEE Vehic. Technol. Conf. (VTC)*, Phoenix, AZ, May. 19977, pp. 1807–1811.

[14] R. Negi and J. M. Cioffi, "Blind OFDM symbol synchronization in ISI channels," *IEEE Trans. Commun.*, vol. 50, no. 9, pp. 1525–1534, Sep. 2002.

[15] J. V. Beek, P. O. Borjesson, M. L. Boucheret, D. Landstrom, J. M. Arenas, P. Odling, C. Ostberg, M. Wahlqvist, and S. K. Wilson, "A time and frequency synchronization scheme for multiuser OFDM," *IEEE J. Select. Areas Commun. (JSAC)*, vol. 17, no. 11, pp. 1900–1914, Nov. 1999.

[16] M. Marey and H. Steendam, "Analysis of the narrowband interference effect on OFDM timing synchronization," *IEEE Trans. Sig. Processing*, vol. 55, no. 9, pp. 4558–4566, Sep. 2007.

[17] M. E. Sahin, I. Guvenc, and H. Arslan, "Opportunity detection for OFDMA-based cognitive radio systems with timing misalignment," *submitted to IEEE Trans. Wireless Commun.*, 2009.

[18] S. K. Wilson, *Orthogonal Frequency Division Multiplexing for Wireless Communications*. Atlanta, GA: Springer Science and Business Media, 2006, ch. 4.2.2, editors: Ye (Geoffrey) Li and Gordon L. Stuber.